AoI-Aware and Persistence-Driven Congestion Control in 5G NR-V2X Sidelink Communications

Alexey Rolich*, Ion Turcanu†, Andrea Baiocchi*
*Dept. of Information Engineering, Electronics and Telecommunications (DIET), University of Rome Sapienza, Italy
†Luxembourg Institute of Science and Technology (LIST), Luxembourg
alexey.rolich@uniroma1.it ion.turcanu@list.lu andrea.baiocchi@uniroma1.it

Abstract—**Congestion control in 5G New Radio (NR) Vehicle-to-Everything (V2X) sidelink communications is a challenging task, mainly due to the distributed nature of the Semi-Persistent Scheduling (SPS) algorithm used in Mode 2 operation. In this paper, we define an adaptive algorithm to set SPS parameters so as to minimize the average Age of Information (AoI) of cooperative awareness messages. The algorithm is based on insights gained from an analytical model of SPS, and its performance is evaluated through simulations. We present initial simulation results demonstrating the convergence and precision of the proposed algorithm, which allows for the rapid attainment of optimal values of Channel Busy Ratio (CBR) and AoI.**

I. Introduction

5G New Radio (NR)-Vehicle-to-Everything (V2X) communication has been designed to support advanced vehicular applications and use cases that go beyond basic safety [1], such as cooperative awareness, perception, and maneuvering [2]. In particular, 5G NR-V2X enables vehicles to extend their perception and awareness beyond the Line of Sight (LOS), i.e., the range of what local sensors such as LIDAR and RADAR can detect. This can be achieved by periodically exchanging messages containing real-time sensor data with neighboring vehicles using Sidelink (SL) communication, a feature introduced in 3GPP Release 16 that allows vehicles to communicate directly without going through the network.

NR-V2X provides two operation modes for SL communication: Mode 1 and Mode 2 [3]. In Mode 1, SL resources are scheduled by the gNodeB in a centralized way, which assumes that all vehicles must be within the coverage of the base station. In Mode 2, the vehicles use the sensing-based Semi-Persistent Scheduling (SPS) algorithm to autonomously select the SL resources in a distributed manner, allowing them to communicate outside the coverage of a gNodeB. Multiple access is based on resource chunks called Sub-Channels (SCs). User data is transmitted over one or more SCs. The SC to be used is initially selected at random from those detected as idle (based on both sensing and signaling carried in the header of SCs, the so called Sidelink Control Information (SCI)). Once an SC is selected, it is kept for a randomized number of times, and is periodically reused. The two key parameters of this persistent randomized multiple access are the usage period, i.e., the Resource Reservation Interval (RRI), and the persistence mechanism, based on the Reselection Counter (RC) and the persistence probability [1].

While NR-V2X Mode 2 has obvious advantages, it is also much more difficult to control the congestion on the communication channel compared to Mode 1, where it is controlled by the gNodeB. 3GPP defines two metrics to measure the channel congestion in NR-V2X SL, that is Channel Busy Ratio (CBR) and Channel occupancy Ratio (CR), but it does not define a specific congestion control algorithm. Several recent works attempt to fill this gap [4]–[6]. For example, Mansouri et al. [4] provide a first analysis of the impact of the Decentralized Congestion Control (DCC) [7] – the mechanism proposed by ETSI to control the congestion in ITS-G5 based V2X networks – on the performance of LTE-V2X Mode 4 (the predecessor of NR-V2X Mode 2). They evaluate the performance of the SPS scheduler in conjunction with DCC, demonstrating that the application of DCC can decrease performance. Toghi et al. [5] also conclude that the simple use of DCC in LTE-V2X SL is not optimal and that further analysis is required to improve the efficiency of the congestion control. Choi et al. [6] instead propose an entirely new DCC mechanism that uses Deep Reinforcement Learning (DRL) to determine the packet transmission rate and control the channel resource utilization. They show that the DRL-based approach improves the Packet Delivery Ratio (PDR) while keeping the CBR close to the target value.

However, these solutions primarily address system-level requirements and overlook application-level concerns such as the Age of Information (AoI) associated with message packets. In fact, AoI has been proposed as a critical application-level performance metric [8] that captures the freshness of update information in V2X systems [9]. It quantifies the environmental sensing gains in cooperative awareness and collective perception, and its application extends to the safety evaluation of automated driving in cooperative maneuvering [10].

While most researchers prioritize the management of the transmission rates or employ hybrid strategies to minimize collisions, only a minority addresses congestion control from the perspective of AoI [7], [11], [12]. In particular, Saad et al. [11] address the congestion issues in 5G NR-V2X SL communication, focusing on scheduling and resource management for advanced applications. They propose a DRL-based congestion control scheme that optimizes Medium Access Control (MAC) layer parameters, considering both system and application requirements, notably AoI. The proposed mechanism is shown to outperform the standard DCC in terms of PDR, average AoI, throughput, and average CBR. Dayal et al. [12] address congestion indirectly by proposing two RRI selection algorithms to improve the tracking error in cooperative awareness applications. They show that combining SPS with either of these approaches outperforms the conventional SPS in all the considered scenarios.

However, none of these previous studies investigate the impact of persistence on congestion control in 5G NR-V2X

© 2024 IEEE. Personal use of this material is permitted. Permission from IEEE must be obtained for all other uses, in any current or future media, including reprinting/republishing this material for advertising or promotional purposes, creating new collective works, for resale or redistribution to servers or lists, or reuse of any copyrighted component of this work in other works.

22nd Mediterranean Communication and Computer Networking Conference (MedComNet 2024)

SL communication. In this paper, we leverage the model defined in our previous work [13] to design an autonomous adaptive algorithm that drives the persistence probability and RRI to values that minimize the average AoI, given the node density. In particular, we identify the optimal system working point that leads to minimal mean AoI, as a function of the persistence probability P and the RRI. We also characterize the optimal working point by analyzing the properties of relevant system quantities, that are then exploited to define a distributed algorithm that drives P and RRI towards the optimal values. We exploit the model defined in [13] to gain insight into the interplay of the key parameters P and RRI and the mean AoI. This insight gives a solid ground to derive the distributed algorithm. Finally, we provide a preliminary evaluation of speed of convergence and accuracy of the algorithm, proving that the distributed algorithm is robust and effective.

As for the rest of the paper, the analysis of the AoI as a function of persistence probability and RRI, the identification of the system working point that minimizes the mean AoI, and the definition of the parameter adaptation algorithm is given in Section II. Numerical results are provided in Section III. Final remarks are presented in Section IV.

II. Model outline and adaptive algorithm

Consider a set of N nodes sharing a 5G NR-V2X communication channel used according to Mode 2 [14]. We aim at identifying the RRI and persistence probability that minimize the mean AoI. To this end we resort to a simplified model that retains the essential characteristics of the SPS algorithm.

We make the following assumptions:

1) Nodes hear each other (no hidden nodes).
2) All nodes use the same RRI.
3) Only broadcast traffic is considered, so no ACK is provided and no retransmission is scheduled.
4) Nodes generate a new message for each RRI.
5) The SC is sized to carry one complete message, i.e., one Transport Block (TB) plus its associated SCI (both first and second stage) fit into one SC.
6) The RC is drawn from a Geometric probability distribution, i.e., $\mathcal{P}(RC = j) = c^{j-1}(1-c)$, for $j \geq 1$. Note that the mean RC is equal to $\overline{RC} = 1/(1-c) \geq 1$, hence c can be identified as $c = 1 - 1/\overline{RC}$.
7) The number of nodes N is less than the number K of SCs available in one RRI.

Assumptions 4 and 5 correspond to the best situation for the SPS algorithm, since message generation is exactly periodic and each new message fits exactly into the reserved resource. Note also that as a consequence of Assumption 7, there is always at least one idle SC in each RRI. Assuming a Geometric Probability Distribution Function (PDF) for the RC is required to derive a Discrete Time Markov Chain (DTMC) model of the system in [13]. The mean RC is adjusted so as to match the average RC setting prescribed by the standard [1]:

$$\overline{RC} = \frac{C \cdot (RC_{\min} + RC_{\max})}{2} \tag{1}$$

with $RC_{\min} = 5$, $RC_{\max} = 15$ and

$$C = \max\left\{1, \min\left\{5, \frac{\mathrm{RRI_{th}}}{\mathrm{RRI}}\right\}\right\} \tag{2}$$

with $\mathrm{RRI_{th}} = 100\,\mathrm{ms}$.

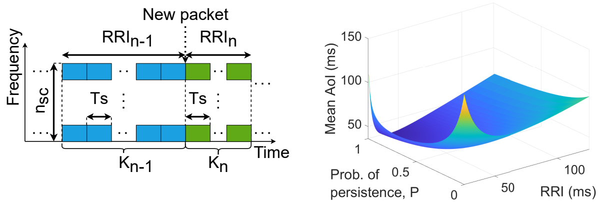

(a) (b)

Figure 1. Characteristics of the communication channel. (a) Channel evolution with adaptive RRI algorithm; (b) Mean of AoI as a function of the probability of persistence P and of the RRI (in ms).

Let K be the number of SCs available in the selection window, i.e., in one RRI. Let n_{SC} denote the number of SCs in a time slot and T_s the time slot time (1 ms with baseline numerology)(structure is shown in Figure 1a). Then, it is

$$\mathrm{RRI} = T_s \left\lceil \frac{K}{n_{\mathrm{SC}}} \right\rceil \tag{3}$$

In each RRI, each node uses one SC to broadcast its message. A node selects an idle SC and persists using it for a number of times equal to its value of RC. Once RC is counted down to 0, the node decides to draw a new value of RC and persist on the same SC with probability P. With probability $1-P$, the node switches to another idle SC and draws a new value of RC.

According to our model assumptions, a node that decides to jump to a new SC selects the target SC uniformly at random among all those SCs that are deemed to be available in the previous RRI. Available means that they have sensed to be idle or that signaling in the SCI tells that the node currently using the SC is using it for the last time and it will jump to another SC in its next RRI.

It is shown in [13] that the mean of the AoI can be evaluated numerically, once the DTMC model is solved resorting to a mean field approximation and a fixed point equation is solved. The result is a function of the three model parameters N, K, and q. The parameter K is directly dependent on the RRI, as seen from Equation (3). The parameter q is directly related to the persistence parameters of SPS, namely $q = (1-P)/\overline{RC}$, where $\overline{RC}$ is given in Equations (1) and (2).

Figure 1b shows the mean AoI $\mathrm{E}[A]$ as a function of P and RRI (expressed in ms) for $N = 100$. It is apparent that there is a global minimum of the AoI. More insight is gained by looking at Figure 2. Figure 2a shows the mean AoI as a function of the system load $\rho = N/K$ (which is implicitly a function of RRI, through K) for $N = 100$ nodes. The solid line curve is obtained by choosing the persistence probability value P^* that minimizes the mean AoI for each value of ρ. The dashed line curve correspond to $P = 0$ (no persistence).

Figure 2b illustrates the probability of success, i.e., the probability that a message sent by a node is correctly decoded by other nodes. In the considered model setting, this is equivalent to saying that no collision occurred, i.e., the node was the only one transmitting in its SC.

The plots in Figure 2 highlight that persistence brings about a substantial performance gain. It also shows that $\mathrm{E}[A]$ has a minimum as a function of ρ. Since we keep N fixed, ρ is varied by changing K, i.e., by changing the value of RRI. For large values of RRI (large K, hence low

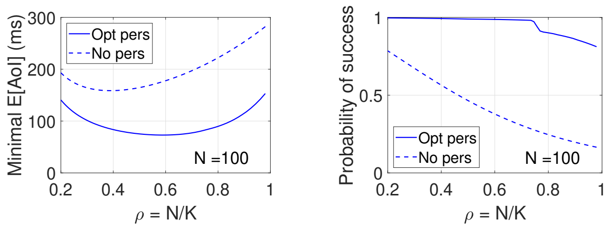

(a) (b)

Figure 2. Performance as a function of the system load $\rho = N/K$, with optimal persistence probability for each value of ρ and for $N = 100$. (a) Mean AoI; (b) Probability of success.

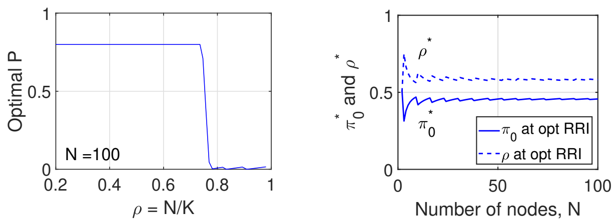

(a) (b)

Figure 3. Characterization of the optimal working point as a function of N. (a) Optimal P as a function of ρ. (b) Probability to find an empty SC π_0 and system load ρ at the optimal working point as a function of $N = 100$.

ρ values), the mean AoI increases since nodes are slack in sending updates, even if the probability of success is very high, thanks to low load. On the other hand, for small values of RRI (hence small K and large ρ values), congestion in the radio interface causes a significant amount of collisions, thus impairing the effectiveness of periodic messaging. As a results, mean AoI deteriorates. The minimal mean AoI is struck for an intermediate value of ρ, hence of RRI.

To gain further insight into the optimal working point to attain minimal mean AoI, we introduce Figure 3. Here, Figure 3a show the optimal value of the persistence probability P as a function of ρ for a fixed number of nodes $N = 100$. Figure 3b illustrates the values of the probability of detecting an empty SC, π_0 and of the system load ρ, evaluated at the optimal working point, i.e., for the optimal persistence probability and the optimal value of RRI. As for the probability of persistence, it turns out that it should be as large as possible (0.8, according to the standard) when we set the system load around the optimal value (≈ 0.6). The plots in Figure 3b shows that, when driving the system to operate so that the mean AoI attains its minimum, the probability of an empty SC π_0 and the system load are both close to constant values, *irrespective of* N, apart from the first few values of N.

Inspired by the results above, we define the Algorithm 1, that each node runs autonomously. The logic of the algorithm can be summarized as follows. The RRI is adapted so as to drive the fraction of idle SCs towards π_0^*, The quantity e_0 measures the distance between the current estimate of this fraction, p_0, and the target value π_0^*. The step size of the adaptation of RRI shrinks as the current RRI R tends towards the optimal value corresponding to $p_0 = \pi_0^*$, hence $e_0 = 0$. To speed up convergence, the persistence probability P is initially set to 0. Then P grows towards the maximum possible value (which has been verified to lead to optimal mean AoI in the first part of this section) as the convergence error e_0 becomes smaller and smaller. The convex sum in the last line of the algorithm averages the adapted value of the RRI R with the average of the RRI of neighbor nodes, R_{nei}. Those values can be read in the SCIs correctly decoded by the considered node over the last W SCs. This final step of the algorithm is key to avoid that RRIs of neighbor nodes scatter over a widely spread out range, while achieving close to the target fraction π_0^* of idle SCs. The value $\tilde{R}$ can be interpreted as the node's *individual* opinion on the current best RRI to get a minimal AoI, while R_{nei} is the *collective* opinion of node's neighborhood. Following $\tilde{R}$ drives the system towards the optimal RRI value. Anchoring to the average of neighbors' RRIs keeps the flock together, avoiding a wide spread of RRI values of neighboring nodes. Balancing the individual and the collective points of view leads the overall system to settle around a unique RRI value that attains minimal mean AoI.

The entire algorithm can be rephrased in terms of CBR, observing that $\text{CBR} = 1 - \pi_0$. Ultimately, the RRI is adjusted so as to drive the CBR towards the optimal value $\text{CBR}^* = 1 - \pi_0^*$, corresponding to minimal AoI.

In the algorithm we set $P_{\text{max}} = 0.8$, $\Delta R = 40$ subframes, $\beta = 0.25$, $\pi_0^* = 0.412$, $\text{RRI}_{\text{min}} = 1$ subframe, $\text{RRI}_{\text{max}} = 1000$ subframes, W = number of SCs in RRI_{max}. Moreover, the upper and lower limits for convergence to π_0^* are $p_{0,\text{sup}} = \pi_0^*(1+\mu)$ and $p_{0,\text{inf}} = \pi_0^*(1-\mu)$, with $\mu = 0.03$.

III. Simulation Results Analysis

In this section, we examine the results of MATLAB-based simulation for the proposed algorithm in scenarios with different numbers of nodes, $N \in \{25, 50, 100, 200\}$. We analyze the evolution of RRI and time-averaged AoI while operating the proposed algorithm. In the simulation, the initial value of RRI is randomly assigned. The value of RC is dynamically determined in accordance with the standard.

Time-averaged AoI is defined as the current average of the instantaneous age of data collected by nodes from other nodes. Formally, it is

$$\langle A \rangle(t) = \frac{1}{t} \int_0^t \text{AoI}(\tau)\, d\tau \tag{4}$$

Figure 4 illustrates the evolution of RRI for randomly selected nodes. We can observe the operation of the proposed adaptive algorithm in achieving an optimal level of RRI and the corresponding optimal CBR. The stepwise change in RRI is explained by the time quantization into subframes. We observe a similar trend in Figure 5, depicting the RRI convergence

Algorithm 1 Algorithm for the adaptation of RRI.

$R \leftarrow \text{RRI}_{\text{th}}$, $P \leftarrow 0$
if New SC must be selected **then**
  $K_0 \leftarrow$ # of idle SCs out of the last W SCs
  $p_0 \leftarrow K_0/W$
  $e_0 = \frac{\max\{0, \pi_0^* - p_0\}}{\pi_0^*} + \frac{\max\{0, p_0 - \pi_0^*\}}{1-\pi_0^*}$
  $P \leftarrow P_{\text{max}}(1 - e_0)$
  if $p_0 > p_{0,\text{sup}}$ **then**
    $\tilde{R} \leftarrow R - e_0 \Delta R$
  end if
  if $p_0 < p_{0,\text{inf}}$ **then**
    $\tilde{R} \leftarrow R + e_0 \Delta R$
  end if
  $\tilde{R} = \max\{\text{RRI}_{\text{min}}, \min\{\text{RRI}_{\text{max}}, \tilde{R}\}\}$
  $R_{\text{nei}} \leftarrow$ average RRI of decoded SCIs over the last W SCs
  $R \leftarrow \beta\tilde{R} + (1-\beta)R_{\text{nei}}$
end if

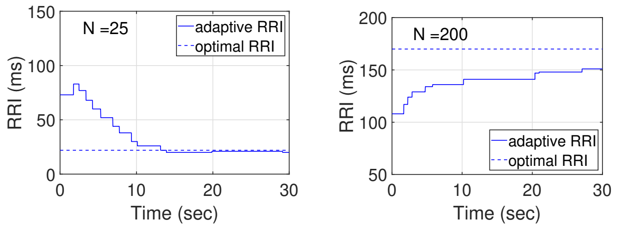

(a) (b)

Figure 4. RRI evolution for random sample node over the time. (a) $N = 25$ (b) $N = 200$.

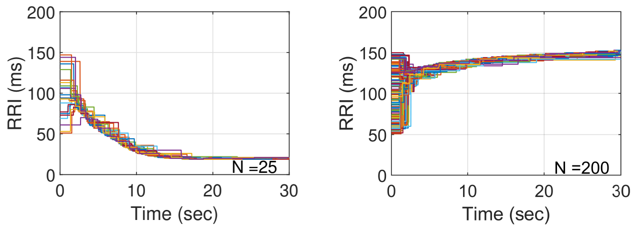

(a) (b)

Figure 5. RRI convergence for all nodes over time with the adaptive algorithm. (a) $N = 25$. (b) $N = 200$.

of all nodes in the network. The utilization of the proposed adaptive algorithm enables rapid attainment of an RRI value nearing the optimal RRI level (convergence occurs within approximately 10 s). To be noted that the proposed algorithm demonstrates high accuracy across various numbers of nodes utilized in the simulation.

Figure 6 illustrates the change in time-averaged AoI over time. The obtained results demonstrate that alongside RRI, AoI convergence occurs rapidly and accurately (correlating entirely with the RRI convergence rate). It is evident that the utilization of the adaptive algorithm minimizes AoI. However, occasional spikes in time-averaged AoI are observed. These spikes are attributed to the imperfections of the SPS algorithm and potential collisions when multiple nodes simultaneously select new resources. Clearly, the frequency and duration of spikes due to collision occurrences increases with the augmentation of nodes in the system (as depicted in Figures 6a and 6b). To be noted that once the adaptive algorithm reaches convergence, it sets the highest possible persistence probability to maintain the optimal point for as long as possible. Nevertheless, situations arise where nodes remain in a collision state for an extended period due to the high persistence probability. Gradually, as nodes exit the collision state, we observe a gradual reduction in time-averaged AoI since AoI is utilized as a metric after a node exits the collision state.

IV. Conclusion

In this paper, we presented an initial investigation into minimizing AoI through dynamic control of persistence probability and RRI. We identified optimal system configurations and proposed a distributed algorithm to achieve them, rooted in a simple yet accurate analytical model. The results underscore the significance of RRI and persistence values on AoI, prompting the development of an adaptive algorithm for DCC. Through simulations, we validated the effectiveness of our approach in quickly attaining optimal CBR and AoI values while addressing accuracy concerns. Future research directions include exploring more complex scenarios and further refining the proposed adaptive algorithm to enhance system performance in realistic scenarios.

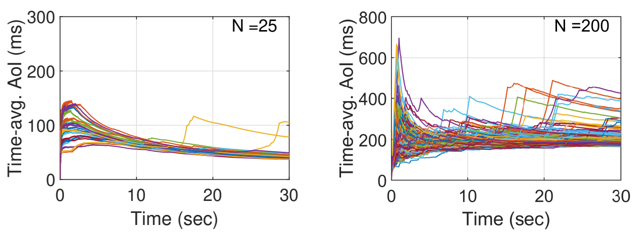

(a) (b)

Figure 6. Time-averaged AoI convergence for all nodes over time with the adaptive algorithm. (a) $N = 25$. (b) $N = 200$.

Acknowledgement

This work was partially supported by the Sapienza University of Rome under the grant n. RP123188F68315A5, project title "Modeling and optimization of sidelink communications in C-V2X 5G NR". The paper was also partially supported by the Luxembourg National Research Fund INTER/ANR/22/17192457/CANDI.

References

[1] M. H. C. Garcia et al., "A tutorial on 5G NR V2X communications," *IEEE Communications Surveys & Tutorials*, vol. 23, no. 3, pp. 1972–2026, 2021.

[2] H. M. Wang, S. S. Avedisov, O. Altintas, and G. Orosz, "Multi-Vehicle Conflict Management With Status and Intent Sharing Under Time Delays," *IEEE Transactions on Intelligent Vehicles*, 2022.

[3] Z. Ali, S. Lagén, L. Giupponi, and R. Rouil, "3GPP NR V2X mode 2: overview, models and system-level evaluation," *IEEE Access*, vol. 9, pp. 89 554–89 579, 2021.

[4] A. Mansouri, V. Martinez, and J. Härri, "A first investigation of congestion control for LTE-V2X mode 4," in *15th Annual Conference on Wireless On-demand Network Systems and Services (WONS)*, IEEE, 2019, pp. 56–63.

[5] B. Toghi, M. Saifuddin, Y. P. Fallah, and M. O. Mughal, "Analysis of distributed congestion control in cellular vehicle-to-everything networks," in *IEEE 90th Vehicular Technology Conference (VTC2019-Fall)*, IEEE, 2019, pp. 1–7.

[6] J.-Y. Choi, H.-S. Jo, C. Mun, and J.-G. Yook, "Deep reinforcement learning-based distributed congestion control in cellular V2X networks," *IEEE Wireless Communications Letters*, vol. 10, no. 11, pp. 2582–2586, 2021.

[7] I. Turcanu, A. Baiocchi, N. Lyamin, and A. Vinel, "An Age-Of-Information Perspective on Decentralized Congestion Control in Vehicular Networks," in *19th Mediterranean Communication and Computer Networking Conference (MedComNet)*, IEEE, Jun. 2021, pp. 1–8.

[8] Z. Chen, N. Pappas, E. Björnson, and E. G. Larsson, "Optimizing Information Freshness in a Multiple Access Channel With Heterogeneous Devices," *IEEE Open Journal of the Communications Society*, vol. 2, pp. 456–470, 2021.

[9] A. Baiocchi, I. Turcanu, N. Lyamin, K. Sjoöberg, and A. Vinel, "Age of Information in IEEE 802.11p," in *17th IFIP/IEEE International Symposium on Integrated Network Management (IM): ITAVT Workshop*, Virtual Conference: IEEE, May 2021.

[10] J. Thunberg, D. Bischoff, F. A. Schiegg, T. Meuser, and A. Vinel, "Unreliable V2X Communication in Cooperative Driving: Safety Times for Emergency Braking," *IEEE Access*, vol. 9, pp. 148 024–148 036, 2021.

[11] M. M. Saad, M. A. Tariq, J. Seo, M. Ajmal, and D. Kim, "Age-of-information aware intelligent MAC for congestion control in NR-V2X," in *Fourteenth International Conference on Ubiquitous and Future Networks (ICUFN)*, IEEE, 2023, pp. 265–270.

[12] A. Dayal, V. K. Shah, H. S. Dhillon, and J. H. Reed, "Adaptive RRI Selection Algorithms for Improved Cooperative Awareness in Decentralized NR-V2X," *IEEE Access*, vol. 11, pp. 134 575–134 588, 2023.

[13] A. Rolich, I. Turcanu, A. Vinel, and A. Baiocchi, "Impact of Persistence on the Age of Information in 5G NR-V2X Sidelink Communications," in *21st Mediterranean Communication and Computer Networking Conference (MedComNet)*, Ponza Island, Italy, Jun. 2023, pp. 15–24.

[14] L. Cao, H. Yin, R. Wei, and L. Zhang, "Optimize Semi-Persistent Scheduling in NR-V2X: An Age-of-Information Perspective," in *2022 IEEE Wireless Communications and Networking Conference (WCNC)*, 2022, pp. 2053–2058.